INSTITUTE OF PHYSICS PUBLISHING SEMICONDUCTOR SCIENCE AND TECHNOLOGY

Semicond. Sci. Technol. **16** (2001) 440–446 www.iop.org/Journals/ss PII: S0268-1242(01)18056-9

Defects and defect behaviour in GaAs grown at low temperature

M Stellmacher[1,3], R Bisaro[1], P Galtier[1], J Nagle[1], K Khirouni[2,4] and J C Bourgoin[2]

[1] Thomson-CSF, Laboratoire Central de Recherches, Domaine de Corbeville, BP 10, 91404 Orsay Cedex, France

[2] Laboratoire des Milieux Désordonnés et Hétérogènes, Université P et M Curie, CNRS, UMR 7603, Tour 22, Casier 86, 4 place Jussieu, 75252 Paris Cedex 05, France

Received 17 October 2000, accepted for publication 27 February 2001

Abstract

We have performed a systematic study of GaAs layers grown at low temperature against the growth temperature and annealing treatments using x-ray diffraction, IR absorption, Hall effect, electron diffraction and Auger spectroscopies. The correlation between the observations obtained with these techniques allowed us to correctly measure the excess As concentration and to show that As antisite related defects can account for all the As in excess. We demonstrate that these As antisites related defects contain two As atoms and we propose a specific model for this defect which explains its disappearance at a relatively low temperature.

1. Introduction

GaAs grown at low temperature, i.e. in a temperature range below the conventional growth temperature (600 °C), is a new type of material which exhibits specific physical properties that are potentially interesting for numerous electronic and optoelectronic applications. This material was first studied for its semi-insulating (SI) property [1, 2]. For instance, it allowed one to eliminate the problem of side-gating [3] in integrated field effect transistors developed on conventional Czochralski (Cz)-grown SI substrates. It is also characterized by a very short lifetime [4, 5]. This property, combined with a high electron mobility and a large dielectric breakdown strength, is used to improve the performance of optoelectronic devices [6, 7] such as high-speed and high-voltage switches and fast wide-band photodetectors.

The properties of this material are directly related to the defects it contains. Information on these defects were obtained using various characterization techniques, but the published data, derived from different samples for each technique, do not provide a coherent picture and a unique defect model accounting for all the observations has not been presented.

During the growth of low-temperature GaAs (LT-GaAs) by molecular beam epitaxy (MBE), arsenic is incorporated in excess as suggested by Auger spectroscopy [8]. It is therefore deduced that, because of the excess As, LT-GaAs contains a high concentration of defects. This is substantiated by x-ray studies which indicate that the lattice parameter has a value larger than that of a defect-free stoichiometric material. As the material is As rich, these defects are assumed to be As interstitials (As_i), As antisites (As_{Ga}), Ga vacancies (V_{Ga}), complexes involving As_{Ga} and As precipitates. It is generally assumed that As_i and two types of As antisites are the dominant defects. In this work, performed on MBE layers grown between 150 and 400 °C, we shall demonstrate that the As excess previously reported has been overestimated so that the dominant defects are only the antisite related defects. It is also recognized that two types of antisite defect exist, one type being stable at high temperature and exhibiting a metastable character, while the other type disappears at a relatively low temperature and is not metastable. We shall demonstrate here that this last antisite contains two As atoms. We shall propose a simple model for the configurations of these two types of antisites, which explain in a coherent fashion their thermal behaviour.

Apart from As precipitates and As antisites, which are directly observed by transmission electron microscopy (TEM) [9] and by scanning tunnelling microscopy (STM) [10] respectively, the existence of other defects is only inferred from the characterization of the material by various techniques. Indeed, none of the techniques taken separately is able to provide a direct identification of a defect, as we shall see in section 2. Each technique provides a piece of information on the nature of a defect, but it is only the correlation between

[3] Current address: Corning SA, Centre Européen de Recherche et Technologie, 7 bis, avenue de Valvin, BP 3, 77211 Avon Cedex, France.

[4] Permanent address: Laboratoire des Semiconducteurs, Faculté des Sciences de Monastir, Route de Kairouan, 5000 Monastir, Tunisia.

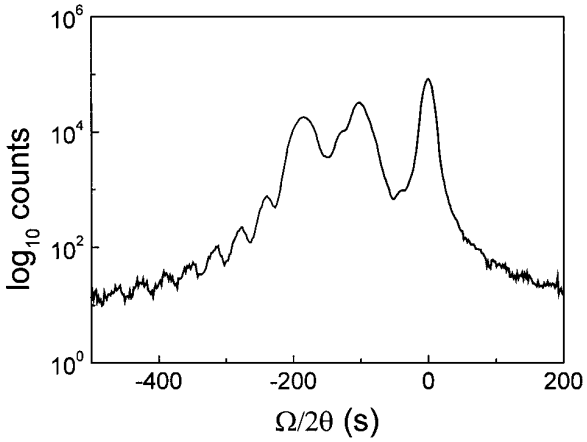

Figure 1. Double x-ray diffraction spectra of a sample containing two LT-GaAs layers: 1 μm grown at 290 °C and 0.5 μm grown at 230 °C. The spectrum exhibits two well defined peaks on the left of the substrate peak. These peaks correspond to lattice mismatches of 7.3×10^{-4} and 1.39×10^{-3} for the layers grown at 290 and 230 °C respectively.

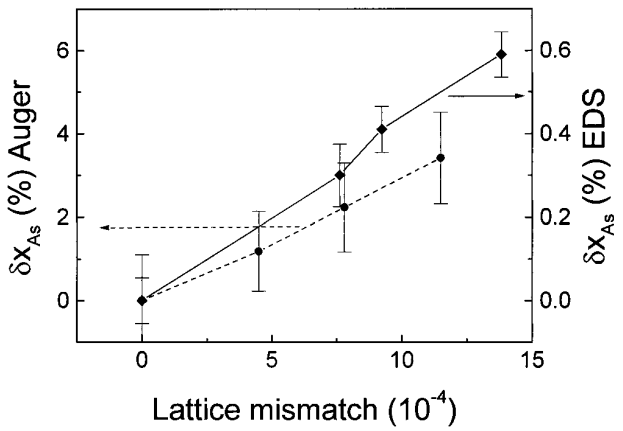

Figure 2. Variation of the excess As for three layers grown at different temperatures against the corresponding lattice mismatch, obtained by EDS (♦) and Auger (●) measurements. Note the different scales.

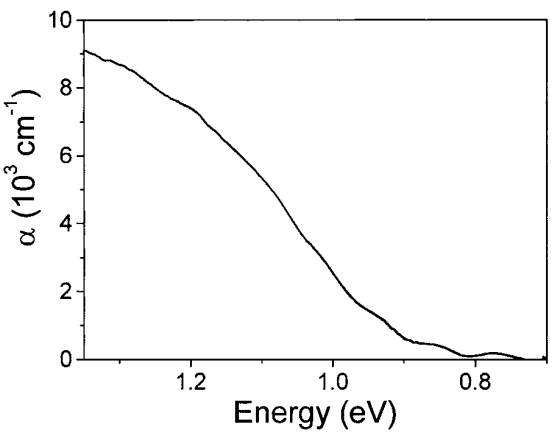

Figure 3. Typical IR absorption spectrum of a 2 μm thick LT-GaAs sample grown at 280 °C. The absorption coefficient at 1 μm is $\alpha = 7.76 \times 10^3$ cm^{-1}.

the information provided by several techniques which can bring a comprehensive picture. Defects submitted to thermal treatments can also give information on their nature through their thermal behaviour.

We therefore present a systematic study of the effect of the growth temperature and of annealing treatments on the nature and concentration of the defects. This study is performed by correlating the results obtained from chemical, structural, optical and electrical techniques on the same materials. We shall see that re-examination of the published data allows one to derive a coherent picture of the defects and shows that all their characteristics can be fitted with a unique and simple model. By performing such a correlation, we shall see that one technique, the one which measures the relative lattice parameter change $\Delta a/a$, is sufficient to characterize a given state of the As related defects in an as-grown layer, i.e. gives a measure of the defect state in a material grown for a given set of growth parameters (arsenic overpressure and growth rate). This result is important because it allows one to make comparisons between different materials grown in different reactors, where the growth temperatures that are measured depend considerably on the way the substrates are mounted in the reactor and on the state (polished or not) of their back surface. The knowledge we acquire on the nature of the defects present in these materials, and on their role on the electronic properties, allows us to determine which defect is sensitive to a specific technique. This provides an improved understanding of the role of the As antisites. Finally, we shall see that only one type of arsenic antisite related defect (AARD) can explain defect rearrangement during thermal treatment and, specifically, the disappearance of the As antisites.

2. Present knowledge

X-ray diffraction demonstrates that GaAs layers grown at low temperature are crystalline and hence contain well defined point defects [8]. The defect concentration is large since high-resolution x-ray diffraction (HRXRD) indicates that the material is characterized by a lattice parameter larger than that of a stoichiometric material [8]. For instance, as illustrated in figure 1, the HRXRD spectrum of a double layer grown first at 290 °C and then at 230 °C shows that the lattice mismatches, $\Delta a/a$, are 1.38×10^{-3} and 7.3×10^{-4} respectively, i.e. are increasing with decreasing growth temperature (see also [8, 11]) as a consequence of a variable concentration of introduced defects.

Auger spectroscopy has been used to measure the As:Ga ratio. The measurements shown in figure 2 are consistent with those already published [8], which stated that As is in an excess of the order of 1%. Because the material is As rich, and because As_{Ga} are observed by STM [10, 12], this lattice mismatch is generally attributed to the presence of these antisites. This attribution is coherent with the observation (see figure 3) of a strong infrared absorption characteristic of a defect related to the As antisite, as we shall see below. However, $\Delta a/a$ could also be, at least partially, attributed to other defects such as the V_{Ga} and As_i, even if theoretical calculations [13] suggest that As_{Ga}, isolated or complexed with As_i, should induce a larger lattice distortion than As_i and V_{Ga}.

After annealing, the lattice parameter relaxes to the standard value of a stoichiometric material. Also, the full-width at half-maximum measured on the (004) Bragg reflection

rocking curve (HRXRD) is lower than 15 arcsec, i.e. close to the value measured on a standard epitaxial layer. Hence, the majority of the defects responsible for the lattice mismatch have disappeared. TEM images of annealed layers then reveal the existence of particles with sizes up to 10 nm [14]. The size and density of these particles vary with the annealing temperature and the growth conditions. High-resolution TEM shows that the associated defects are spherical precipitates and that the atoms in the precipitates have a crystalline structure. Melloch *et al* [14] identified the nature of the atoms as being As. Such As precipitates are only detectable after annealing, but it is likely that smaller precipitates exist, undetectable because of their size for the lowest annealing temperatures. After annealing, all defects have disappeared (or are at least at a concentration lower than 10^{18} cm^{-3}) and the volume fraction occupied by the As precipitates is smaller than that expected if all the excess As has been removed.

Infrared absorption at 1 μm is commonly used to detect the so-called EL2 defect, known to be associated with As_{Ga} [15], and to measure its concentration [16] in SI materials. The same absorption is also used in LT-GaAs to conclude that this material contains a large concentration of the same defect [2]. However, only a small fraction (10%) apparently exhibits the typical photoquenching behaviour of the EL2 defect [2] and the use of the absorption to measure the concentration of the defects is an approximation. There exist at least two different AARDs, sometimes called 'EL2 like', which all give rise to near midgap levels. The absorption at 1 μm can be considered as an average evaluation of their total concentration (deep defects in GaAs are characterized by a large electron–phonon interaction which induces overlap of the absorption bands related to neighbouring energy levels). The existence of these EL2-like defects was first inferred from Hall effect measurements. From the temperature dependence of the free electron concentration, the position of the Fermi energy in the band gap is found to be lower in LT-GaAs than in Cz SI material (where the Fermi level is pinned on the EL2 level at 0.75 eV below the conduction band). It was then argued that the Fermi level in LT-GaAs is pinned on another EL2-like defect [1].

Because the defects exhibit slightly different electrical characteristics [17, 18] from those of the EL2 defect and are observed to disappear at a relatively low temperature (400 °C), while in SI Cz grown material the EL2 defect remains stable above 1000 °C, it must be concluded that there are two types of AARD [18, 19]. Finally, IR absorption follows the same pattern as $\Delta a/a$ against the temperature of growth [11], suggesting that both techniques are sensitive to the same defect. This is, however, not fully established because the two techniques could be sensitive to two different defects whose relative concentrations remain constant when the growth temperature varies.

There are also point defects, other than the AARDs. Positron annihilation [20] indicates the existence of vacancy related defects, but we cannot decide if these vacancy defects are isolated, Ga or As vacancies, or vacancy complexes. Moreover, the technique suggests that their concentration is high, but cannot be measured. Finally, electron paramagnetic resonance provides essentially similar information [21], namely that intrinsic defects exist in large concentration. All intrinsic defects in GaAs give rise to similar spectra because As and Ga atoms possess the same nuclear spins ($\frac{1}{2}$), and different defects could only be differentiated if their hyperfine interactions were known, which is not the case. Optical detection of magnetic resonance suffers the same drawback (see [15] for a discussion concerning the EL2 defect).

In conclusion, the knowledge of the defects contained in LT-GaAs is limited. Their nature has not been firmly established, except for the As precipitate. The existence of the As_{Ga} related defect has been established, but its exact nature is still unknown. It could be an isolated As antisite, or an antisite in a situation that modifies its electronic and optical characteristics. It is admitted that IR absorption and $\Delta a/a$ have to be ascribed to the existence of AARDs, but it is not known if the relationship is a direct one. Liu *et al* [11] noticed that the IR absorption at 1 μm is proportional to $\Delta a/a$ and they concluded that the defect detected by HRXRD is As_{Ga}. However, they have only proven that the defects seen by these two techniques are incorporated in the same proportion during growth at different temperatures. Moreover, As_{Ga} is not the only defect present: As_{Ga}–As_i complexes, i.e. isolated As_{Ga} slightly perturbed by the presence of As_i, could also perhaps induce a similar IR absorption [13] and their concentration could be proportional to As_{Ga}. Hence, the results of Liu *et al* would be identical if HRXRD was sensitive to As_i and if the incorporation of As_{Ga} measured by IR absorption was proportional to the incorporation of As_i.

The aim of this work is to describe new observations performed in order to answer some of the above questions, in particular to obtain a better knowledge of the AARDs and to recognize and describe the behaviour of the interstitial As. For this we first provide a correct evaluation of the amount of excess As. We then correlate data obtained by IR absorption, Hall effect and HRXRD as functions of the growth and annealing temperatures. This correlation permits us to conclude that each of these techniques gives information on the same defect, the AARD. We demonstrate that the amount and kinetics of AARD disappearance, in connection with the growth of precipitates, makes it possible that only one single model for the nature of the AARD is able to physically explain all the observations and hence to solve the contradictions concerning the amount of excess As and the apparent instability of the As antisites.

3. Sample growth

The samples studied in this work have been grown in a Varian Gen II MBE system. An As_4 solid source was used. The growth temperature was controlled with a thermocouple. For reproducible substrate temperatures, the same molyblock was used for all the growths, performed on double-side polished substrates. The growth rate was determined by RHEED oscillations at the substrate temperature. The ratio R of the As_4 and Ga fluxes was calibrated by the determination of the transition point between the (2 × 4) As and the (4 × 2) Ga stabilized reconstruction at a substrate temperature of 550 °C, measured with a pyrometer. In this work, when no specific precision is given, the growth rate is 1 μm h^{-1} and the flux ratio is $R = 2.2$ with this growth chamber. With the above growth parameters, a thermocouple indication of 280 °C corresponds to a lattice mismatch of 1.39×10^{-3}.

4. Results

We first examined the amount of excess As using energy diffraction spectroscopy (EDS). For this we used the 30 keV electron beam of a scanning electron microscope, with an intensity of 10^{-10} A and a 1 μm diameter (electrons with energies larger than few hundred kiloelectronvolts are necessary to produce defects). The penetration depth of such a beam in GaAs is about 1 μm, i.e. of the order of the layer thickness (2 μm). The x-ray photons which are emitted are collected and analysed (1–300 counts s^{-1} over 6×10^3 s). The ratio between the x-ray signal characteristics of the Ga and As, normalized to the ratio observed with a standard GaAs layer, gives the fraction of the gallium and the arsenic atoms inside the LT-GaAs layer and thus the variation of stoichiometry. Figure 2 gives the results obtained for three as-grown layers against their lattice mismatch.

We also performed Auger measurements using a PHI 680 field emission scanning Auger nanoprobe. For this experiment, the primary electron beam, of diameter 0.8 μm and intensity 2×10^{-11} A, was accelerated at 5 keV. The secondary electrons emitted by the Ga and As atoms were analysed as in the EDS experiment, the stoichiometry being deduced from the variation of the ratio between the As and the Ga electrons. The results are also given in figure 2. Examination of this figure allows one to conclude that the EDS results are different from the Auger ones. This is because EDS probes the volume of the layer, while Auger spectroscopy is sensitive to the surface. The Ar ion beam, used to sputter the surface and make depth profiling in the Auger experiment, perturbs the surface stoichiometry: the As atoms being preferentially sputtered, the surface is Ga rich [22]. We can therefore conclude that the stoichiometry of the surface probed by Auger measurements is not that of the volume, as it is in the case of EDS. The correct stoichiometry is therefore that given by EDS. As shown in figure 3, the As in excess is five times lower than previously claimed.

We now examine the correspondence between the lattice mismatch and IR absorption. The absorption of the layer, illustrated in figure 3, is obtained after subtracting the contribution of the substrate. Figure 4 shows that the direct relationship between the quantities $\Delta a/a$ and α, the absorption coefficient at 1 μm, is the same when the defect concentration varies with the growth temperature (as already established in [11]) but also during isochronous or isothermal annealings. This demonstrates that the relative concentrations of the defects detected by these two techniques remain constant during annealing as well as during growth. The proportionality between $\Delta a/a$ and α observed during annealing demonstrates that both are characteristics of the same annealing kinetics and hence are sensitive to the same defect. Because all AARDs give rise to the same absorption as the EL2 defect (see section 2), we use the IR absorption calibration for the concentration of this last defect [16] from which we deduce the proportionality between α and $\Delta a/a$:

$$\alpha\ [\mathrm{cm}^{-1}] = 1.08 \times 10^7 \Delta a/a \qquad (1)$$

which allows to deduce directly the AARD concentration from the measurement of $\Delta a/a$.

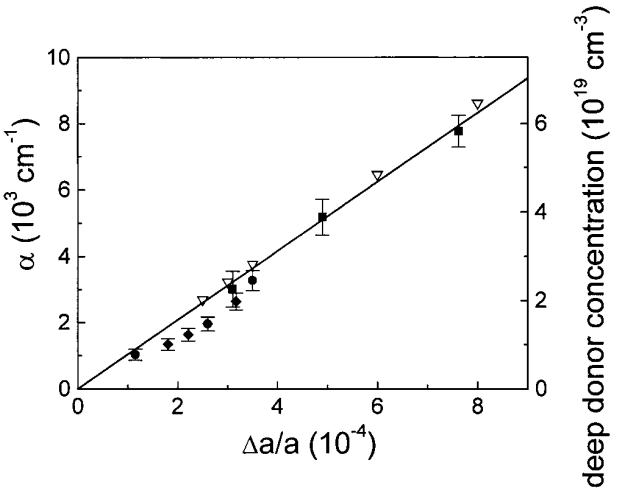

Figure 4. Relative change in the absorption coefficient at 1 μm plotted against the lattice parameter change for layers grown at 280, 300 and 320 °C (■); for layers grown at 280 °C and annealed at 475, 500, 550 and 600 °C for 60 s (●); for layers grown at 280 °C and annealed at 500 °C for 30, 60, 120 and 300 s (♦). The data of [14] are indicated by (▽). The corresponding AARD concentration deduced from the calibration of [16] is also given.

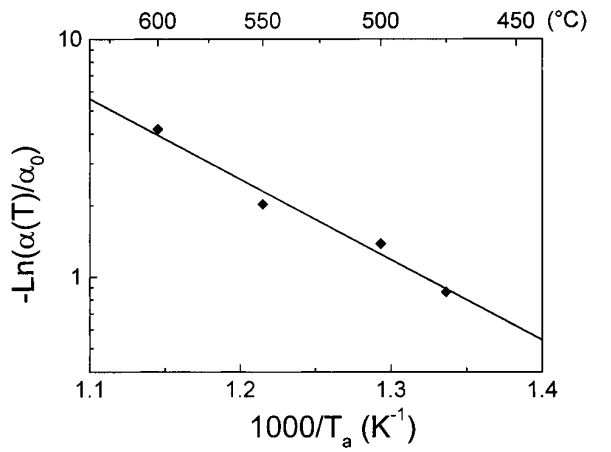

Figure 5. Variation of the absorption coefficient at 1 μm normalized to the unannealed value α_0 (7.76×10^3 cm^{-1}), against the inverse of the annealing temperature for a 60 s anneal. The measurements were performed on a sample grown at 280 °C. In a diffusion limited precipitation, the slope of this plot (0.66 eV) is $3E_m/2$.

Annealing kinetics provide other information. It has already been demonstrated [23], based on TEM observations, that the formation of As precipitates results from diffusing As_i. This conclusion is fully verified here, using α and $\Delta a/a$ data. The annealing kinetics monitored by IR absorption and HRXRD are characterized by the same activation energy: $E_m = 0.44$ eV, as shown in figure 5. The low value of the measured migration energy, E_m, indicates that the annealing kinetics do not involve a substitutional impurity defect, such as As_{Ga}, for which the activation energy for diffusion is several electronvolts [24]. The mobile As defect is therefore an interstitial, As_i. This assignment for E_m is coherent with the activation energy associated with annealing, measured in ion implanted [25] as well as in electron irradiated [15] materials. The annealing reaction is indeed limited by diffusion since, as shown in figure 6, for long enough annealing times the time

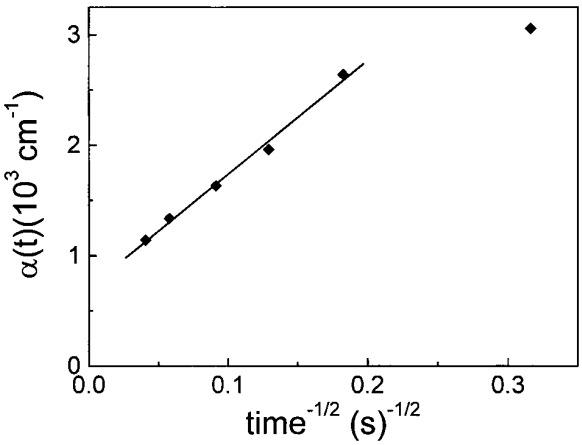

Figure 6. Variation of the absorption coefficient at 1 μm against the inverse of the square root of the annealing time. The measurements were made on a sample grown at 280 °C and annealed at 500 °C.

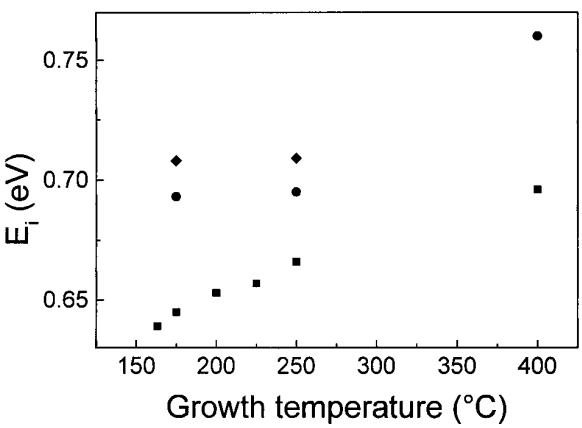

Figure 7. Variation of the ionization energy of the deep donor level in LT-GaAs as a function of growth and annealing temperatures for unannealed layers (■), and for 600 °C annealed layers for 30 min (●) and 10 h (⧫).

dependence of the remaining fraction of the diffusing species varies as $t^{-1/2}$ [26].

The regime of electrical conduction at low temperature is hopping, due to the existence of a partially filled band induced by the defects. Such a conduction regime implies that the Fermi level is located inside the defect band. Above room temperature the electronic conduction is induced by the ionization of electrons from the defects, which then dominates hopping conduction [18]. Hence, the ionization energy E_i associated with the conduction electrons, in concentration n determined by the slope of $\log n$ against T^{-1}, is a measure of the energetic location of this defect band. Figure 7 gives the variation of E_i against the growth temperature and the annealing treatments. It shows that E_i increases when the growth temperature increases. This value is further increased with the time of annealing. Figure 7 demonstrates, therefore, that E_i tends to reach a value of the order of 0.72 eV when the growth temperature, or the time of annealing, increases, i.e. when the concentration of the AARDs decreases.

Assuming that the variation ΔE_i of E_i is induced by the Coulombic interaction between AARDs, ΔE_i can be calculated as a function of the defect concentration C; it is

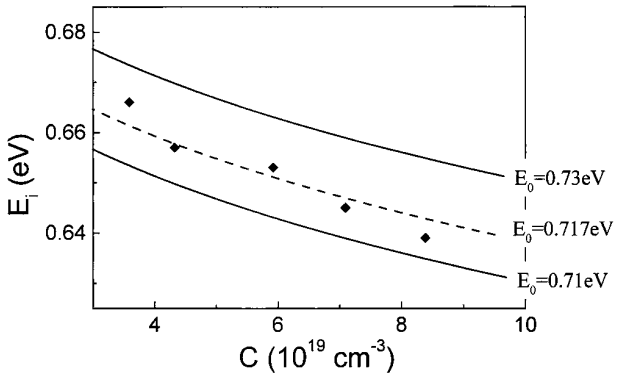

Figure 8. Variation of the ionization energy against the deep donor concentration determined by x-ray measurements. The correspondence between the lattice parameter and the deep donor concentration given in figure 4 was used. The curves are fits for different values of E_0.

given by

$$\Delta E_i = e^2/\varepsilon R \tag{2}$$

where

$$R = (3C/4\pi)^{-1/3} \tag{3}$$

is the average distance between the defects. The dependence of the AARD concentration C, measured by HRXRD and using the established correlation with IR absorption, allows us to derive $E_i(C)$. Figure 8 demonstrates that the experimental data fit the calculated variation of ΔE_i when one takes $E_0 = 0.72$ eV for the ionization of the isolated defect. Thus the observed change in the apparent ionization energy of an AARD is a consequence of the electrostatic interaction between adjacent defects. This conclusion is therefore an indication, like the IR absorption observation, that the defects involved are AARDs which exhibit an ionization energy perhaps slightly lower than that of the EL2 defects (0.75 eV).

In conclusion, the defects appear to be AARDs whose electronic characteristics are very close to those of the EL2 defect and are perturbed by electrostatic interaction. The annealing study allows us to conclude that As precipitates grow at the expense of the AARDs. Moreover, the migrating entity, As_i, is responsible for both the formation of As precipitates and the disappearance of the AARDs which constitute the source of the As_i.

5. Discussion

Low-temperature grown GaAs is a crystalline material containing a high concentration of point defects, resulting from the presence of As in excess. This excess of As is in fact not as high as previously claimed, based on Auger spectroscopy data. The excess As is under the form of As antisites, labelled here AARDs; but the exact nature of these antisites is still unknown. The thermal treatments demonstrate that the AARDs disappear around 400 °C while EL2 defects are stable up to high temperatures (at least 1000 °C) in SI materials. Hence, we have to derive a model for an AARD, which can explain that it anneals at low temperature, while releasing a mobile As_i, the entity which induces the formation of As precipitates:

$$\text{AARD} \rightarrow \text{mobile } As_i \rightarrow \text{As precipitates.} \tag{4}$$

For the sake of clarity, we consider first the isolated antisite. It anneals through the reaction

$$As_{Ga} \rightarrow As_i + V_{Ga}. \quad (5)$$

However, this reaction cannot take place around 400 °C since impurity diffusion, such as self-diffusion, occurs only at much higher temperatures, 1000 °C or above [24].

We then consider the As_{Ga} complexed with an As_i [13], noted (As_{Ga}, As_i), formed by the association of an isolated As_{Ga} and an As_i. Such a complex could anneal at a rather low temperature by the dissociation of its elements:

$$(As_{Ga}, As_i) \rightarrow As_{Ga} + As_i. \quad (6)$$

This reaction can explain the observed low-temperature annealing. However, it cannot explain that, after this reaction has taken place, isolated As_{Ga} have not disappeared, as indicated by IR absorption.

We now consider that the (As_{Ga}, As_i) complex exhibits a new configuration, i.e. becomes a new defect involving two As atoms. It is presumably a split configuration [13], which we note $(As–As)_{Ga}$, in which the two As atoms occupy symmetric sites centred at the Ga site. In such a case the annealing reaction is expected to be

$$(As–As)_{Ga} \rightarrow 2As_i + V_{Ga}. \quad (7)$$

When As_i are mobile they can precipitate following reaction [4], but they also form antisites when being trapped by Ga vacancies:

$$As_i + V_{Ga} \rightarrow As_{Ga}. \quad (8)$$

However, according to [13], a split configuration should possess an electronic structure very different from that of the isolated antisite and should not give rise to similar Hall effect and IR absorption observations. This model should therefore also be ruled out.

These considerations lead one to consider a combination of the two situations alone in order to explain the disappearance of As_{Ga} during thermal treatment. Annealing takes place in two steps. The first step is a transformation of the defect configuration, the original one consisting of an As_{Ga} perturbed by the presence of an As_i:

$$(As_{Ga}, As_i) \rightarrow (As–As)_{Ga}. \quad (9)$$

The split configuration then anneals through reaction (7). A fraction of the released As_i form precipitates (reaction (4)) while the remaining fraction form isolated antisites (reaction (8)) and, finally, new complexes through the reaction

$$As_{Ga} + As_i \rightarrow (As_{Ga}, As_i). \quad (10)$$

The same pattern (reactions (9), (7), (4) and (10)) takes place again, and the end of the annealing corresponds to the exhaustion of As_i. The remaining As precipitates and isolated As_{Ga} are in low concentrations, but still high enough to make the material SI.

Note that in this model the annealing is not limited by reaction (9). Indeed, the activation energy E_m associated with annealing must be ascribed to the As_i mobility from independent observations and because the annealing is dominated by a diffusion process. Hence the experimental data are compatible with AARDs being (As_{Ga}, As_i) complexes and not isolated As_{Ga}.

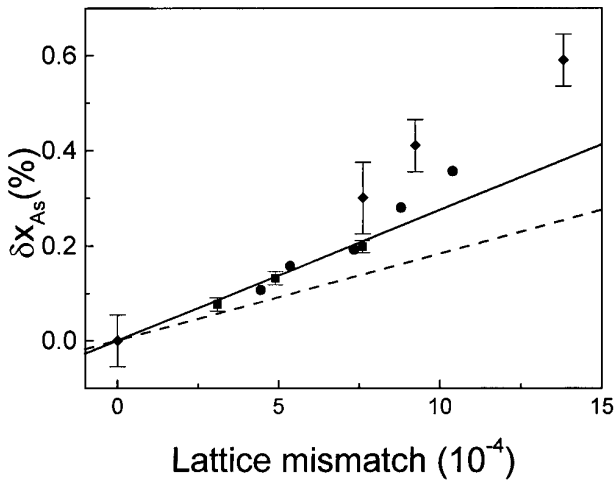

Figure 9. Variation of the stoichiometry as deduced from EDS (♦) against the lattice mismatch and deduced from IR absorption (■) and Hall (●) measurements. The full and the broken lines represent the variations expected when the AARD defect contains two or one As atom, respectively.

We now discuss the observations made in terms of this model in order to check its validity. We have developed three methods to quantitatively measure the concentration of AARDs, which are in fact (As_{Ga}, As_i) complexes. They are measurements of the stoichiometry by EDS, of the IR absorption and of the ionization energy E_i. Since IR absorption and E_i measure the concentration, C, of a defect which involves two As (an As_{Ga} and an As_i), this concentration induces a stoichiometric variation x ($Ga_{1-x}As_{1+x}$) equal to $x = 3C/4C_0$ ($C_0 = 2.2 \times 10^{22}$ cm^{-3} is the Ga or As concentration in Ga_{As}). Indeed, the stoichiometric variation is $x = C/C_0$, when induced by C interstitials, and $x = C/2C_0$, when induced by C isolated antisites. Hence in the model considered here of an AARD involving to As atoms, a linear relationship should exist between x and C, with the coefficient β slope of C against x equal to 3.4×10^{-23} cm^{-3}. If the AARDs are isolated antisites, this coefficient β should be 2.3×10^{-23} cm^{-3}. We now check if a coherence between all the measurements exists and we determine experimentally the proportionality coefficient β. Figure 9 presents the stoichiometric variation calculated from IR absorption and ionization energy measurements as a function of the lattice mismatch. These results are also compared to the direct EDS measurements. Figure 9 demonstrates that all three methods give the same magnitude for the AARD concentration, which also corresponds to the estimated concentration deduced from the precipitate volume fraction after a long annealing time. From figure 9, we deduce $\beta = 3.7 \times 10^{-23}$, thus confirming that an AARD contains two As atoms.

The slight difference (less than 25%) observed between IR absorption and EDS measurements can be explained in terms of the difference between the optical cross sections of the AARD and of the isolated As_{Ga}. Another source of discrepancy can be the fraction of the AARDs in the split configuration and/or

the presence of As_i that are not detected by the IR absorption experiments.

6. Conclusion

With this work we have obtained a reasonable understanding of the defects and of their behaviour in GaAs grown at low temperatures. We have demonstrated that the main defect is the As antisite complexed with an As interstitial. Because the excess As concentration is of the order of 0.1% and not 1%, as was previously thought, the observed concentration of these (As_{Ga}, As_i) complexes can account for most of the As excess. The variation of their electronic characteristics with the conditions of growth is understood in terms of Coulomb interactions between defects. When the dissociation of the (As_{Ga}, As_i) complex takes place, As_i are liberated, diffuse and induce As precipitation. We have shown that the (As_{Ga}, As_i) dissociation must necessarily occur via the formation of an intermediate 'split' configuration such that its dissociation leads to liberation of two As_i. Using this model a coherent picture of the defect behaviour during growth and annealing is obtained. The validity of the model is confirmed by the fact that a quantitative agreement with experiment is obtained for all physical measured parameters, namely IR absorption, electrical properties and the amount of excess As.

References

[1] Look D C, Walters D C, Manasreh M O, Sizelove J R, Stutz C E and Evans K R 1990 *Phys. Rev.* B **42** 3578

[2] Manasreh M O, Look D C, Evans K R and Stutz C E 1990 *Phys. Rev.* B **41** 10 272

[3] Smith F W, Calawa H R, Chen C L, Mantra M J and Mahoney L J 1988 *IEEE Electron. Device Lett.* **9** 77

[4] Viturro R E, Melloch M R and Woodall J M 1992 *Appl. Phys. Lett.* **60** 3007

[5] Gupta S, Frankel M Y, Valdmanis J A, Whitaker J F, Smith F W and Calawa A R 1991 *Appl. Phys. Lett.* **59** 3276

[6] Chen Y, Williamson S, Brock T, Smith F W and Calawa A R 1991 *Appl. Phys. Lett.* **59** 1455

[7] Motet T, Nees J, Williamson S and Mourou G 1991 *Appl. Phys. Lett.* **59** 1455

[8] Kaminska M, Liliental-Weber Z, Weber E R, George T, Kotright J B, Smith F W, Tsaur B-Y and Calawa A R 1989 *Appl. Phys. Lett.* **54** 1881

[9] Melloch M R, Otsuka N, Woodall J M, Warren A C and Freeouf J L 1990 *Appl. Phys. Lett.* **57** 1531

[10] Feenstra R M, Woodall J M and Pettit G D 1993 *Phys. Rev. Lett.* **71** 1176

[11] Liu X, Prasad A, Nishio J, Weber E R, Liliental-Weber Z and Walukiewicz W 1995 *Appl. Phys. Lett.* **67** 279

[12] Feenstra R M, Vaterlaus A, Woodall J M and Pettit G D 1993 *Appl. Phys. Lett.* **63** 2528

[13] Landman J I, Morgan C G, Schick J T, Papoulias P and Kumar A 1997 *Phys. Rev.* B **55** 15 581

[14] Melloch M R, Nolte D D, Otsuka N, Chang C L and Woodall J M 1993 *J. Vac. Sci. Technol.* B **11** 795

[15] Bourgoin J C, von Bardeleben H J and Stievenard D 1988 *J. Appl. Phys.* **64** R65

[16] Martin G M 1981 *Appl. Phys. Lett.* **39** 747

[17] Goo C H, Lau W S, Chong T C and Tan L S 1996 *Appl. Phys. Lett.* **69** 2543

[18] Fang Z Q and Look D C 1993 *J. Electron. Mater.* **22** 1429

[19] Kowalski G, Kurpiewski A, Kaminska M and Weber E R 1993 *Mater. Sci. Eng.* B **22** 27

[20] Gebauer J, Kraux-Rehberg R, Eichler S, Luysberg M, Sohn H and Weber E R 1997 *Appl. Phys. Lett.* **71** 638

[21] Reinacher N M, Brauldt M S and Stutzman M 1995 *Mater. Sci. Forum* **196–201** 1915

[22] Malherbe J B, Banard W O, Strydom I and Louw C W 1992 *Surf. Interface Anal.* **18** 491

[23] Bourgoin J C, Khirouni K and Stellmacher M 1998 *Appl. Phys. Lett.* **72** 442

[24] Tuck R 1988 *Diffusion in III–V Compounds* (Stevenage: Peregrinus)
Casey H C Jr 1973 *Atomic Diffusion in Semiconductors* ed D Shaw (London: Plenum)

[25] Nishizawa J, Shiota I and Oyama Y 1986 *J. Phys. C: Solid State Phys.* **19** 1

[26] Bourgoin J C and Lannoo M 1983 *Point Defect in Semiconductors: Experimental Aspects* vol 2 (Berlin: Springer) ch 9